Supporting Information For

Quasi-Resonance Signal Amplification By Reversible Exchange

Thomas Theis,[a,b] Nuwandi M. Ariyasingha,[c] Roman V. Shchepin,[d] Jacob Lindale,[b] Warren S. Warren,[b] Eduard Y. Chekmenev*[c,e]

[a]Department of Chemistry, North Carolina State University, Raleigh, North Carolina, 27695-8204, United States

[b]Department of Chemistry, Duke University, Durham, North Carolina, 27708, United States

[c]Department of Chemistry, Integrative Biosciences (Ibio), Wayne State University, Karmanos Cancer Institute (KCI), Detroit, Michigan, 48202, United States

[d]Vanderbilt University Institute of Imaging Science (VUIIS), Department of Radiology and Radiological Sciences, Nashville, Tennessee, 37232-2310, United States

[e]Russian Academy of Sciences, Leninskiy Prospekt 14, Moscow, 119991, Russia

Table of Contents

1. Computations of ^{15}N signal enhancement and polarization levels

Computation of signal enhancements was very challenging at 0.05 T, because even highly concentrated sample would not provide any signal. Therefore, the signal enhancements were computed using lower limit estimate as the following.

Metronidazole-$^{15}N_2$-$^{13}C_2$: The highest SNR achieved was 1,270 at 20 mM concentration (Figure 4c). The concentration of ^{15}N spins in signal reference sample (imidazole-$^{15}N_2$ prepared as described previously[1]) was ~8 M in D_2O. The reference sample was placed in conventional standard-wall 5 mm NMR tube. Note the reference sample contain two labeled ^{15}N sites. SNR of at least 2 is required to see any signal, but no signal was observed with 16 scans (square root of 16 is 4 for SNR purpose calculation). 1.85 is a factor related to different effective cross-section of the NMR tubes in HP and thermally polarized experiments.[2]
Assuming that both ^{15}N sites were polarized by QUASR-SABRE in metronidazole-$^{15}N_2$-$^{13}C_2$: we arrive to

ε_{15N} = ((√# of scans reference)/(√# of scans HP sample))*((HP SNR)/(SNR Reference))*1.85*([reference]/[hyperpolarized sample])*((# of ^{15}N sites per molecule in reference sample)/(# of ^{15}N sites per molecule in HP sample)) = (√16/√8)*(1,700/2)*1.85*[8/0.02]*[2/2] = $9.0*10^5$
Note this is the lower limit of signal enhancements, because we do not know how low thermal reference truly is.
^{15}N thermal polarization at 49 mT and 298 K is $1.7*10^{-6}$%.
Therefore, $\%P_{15N} = \%P_{thermal}*\varepsilon_{15N} = 1.7*10^{-6}\%*9.0*10^5=1.5\%$
However, if only one ^{15}N site was polarized, the number below would be effectively doubled!

The integral signal value in Figure 4a (SABRE-SHEATH) is **0.162**. The integral signal value in display Figure 4c (QUASR-SABRE) is **0.394**.

Next, using integral values we arrive to the following numbers for SABRE-SHEATH:

$\varepsilon_{15N} = 9.0*10^5*(0.162/0.394) = 3.7*10^5$ with $\%P_{15N}$ ~ 0.6%

One again, these are the lower limit numbers.
Note, under similar conditions, the average ^{15}N polarization using high-field NMR spectroscopy for SABRE-SHEATH on metronidazole-$^{15}N_2$-$^{13}C_2$ was 1.4%.[3] These numbers are somewhat similar, which is a good news.

The efficiency defined as S(QUASR-SABRE)/S(SABRE-SHEATH) = 2.43!

Note if we are polarizing only one site via QUASR-SABRE versus two ^{15}N sites in SABRE-SHEATH, the

efficiency is doubled to 4.86!

Pyridine-^{15}N: Using the numbers above we can also compute lower-limit values for ^{15}N signal enhancement and polarization values for pyridine-^{15}N for both SABRE-SHEATH and QUASR-SABRE (since the integral numbers are similar: **0.143** and **0.145** for Figure 2a and Figure 2c respectively):

ε_{15N} = ([metronidazole-$^{15}N_2$-$^{13}C_2$]/[pyridine-^{15}N])*((# of ^{15}N sites in metronidazole-$^{15}N_2$-$^{13}C_2$)/(# of ^{15}N sites in in pyridine-^{15}N))*((integral signal value of pyridine-^{15}N)/(integral signal value of metronidazole-$^{15}N_2$-$^{13}C_2$))* ε_{15N} (metronidazole-$^{15}N_2$-$^{13}C_2$) = (20/20)*(2/1)*(0.145/0.394)*$9*10^5$ = $6.6*10^5$ with $\%P_{15N}$ ~ 1.1%.
Again, this is not far from what is expected in this concentration range.[4-5]

<u>Acetonitrile-^{15}N</u>: Using the numbers above we can also compute low-limit values for ^{15}N signal enhancement and polarization values for acetonitrile-^{15}N for both SABRE-SHEATH (Figure 3a, signal integral value of **0.0525**) in a manner similar to that for pyridine-^{15}N calculation detailed above:

$\varepsilon_{15N} = (20/40)*(2/1)*(0.0525/0.394)*9.0*10^5 = 1.2*10^5$ with $\%P_{15N} \sim 0.2\%$.

And for and QUASR-SABRE (Figure 3c, signal integral value of **0.0230**):

$\varepsilon_{15N} = (20/40)*(2/1)*(0.023/0.394)*9.0*10^5 = 5.3*10^4$ with $\%P_{15N} \sim 0.09\%$.

2. Details of shaped SLIC RF pulse preparation

The rectangular ^{15}N RF pulse was calibrated on a hyperpolarized sample prepared via SABRE-SHEATH approach at 210.0 kHz resonance frequency. The calibration yielded a value of $t_{90°}$ = 260 μs at -33 db of power setting. This value corresponded to ~ 960 Hz of B_1 power or ($\omega_1/2\pi$). The TOMCO RF amplifier was deemed to be linear all the way to -48 db (Figure S4c). As a result, the power setting employed (-40 db for all experiments) had a B_1 power of (960/2.24) = 430 Hz.

The SLIC pulse was designed in 100 equally spaced steps with the amplitude starting from 1.00, 0.99, 0.98,…, 0.01 as a table. The shape of the RF pulse was tested on the oscilloscope. We note a minor droop in power at the end of the shaped pulse related to the RF amplifier non-linearity at very low power settings.

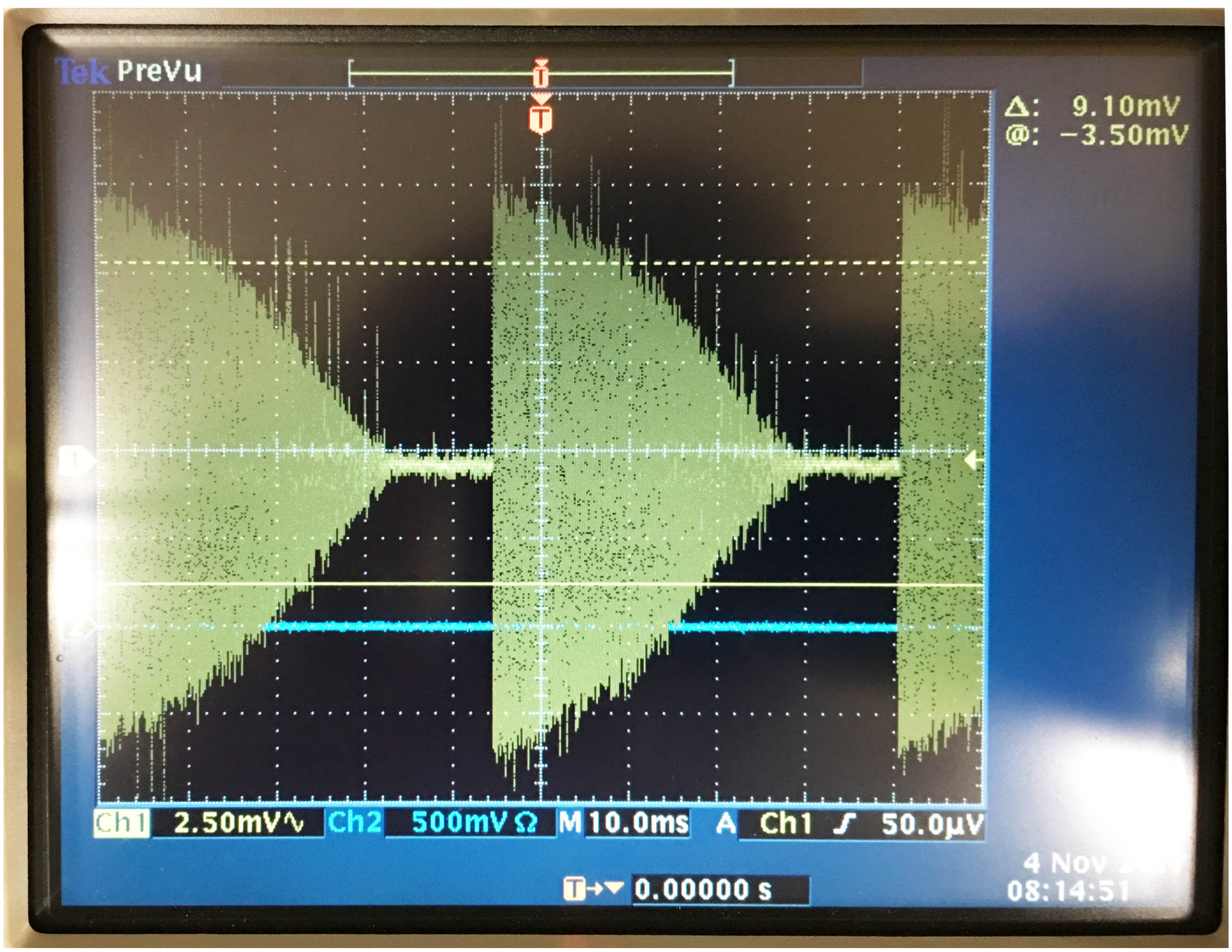

Figure S1. The photograph of two shaped pulse on the digital oscilloscope.

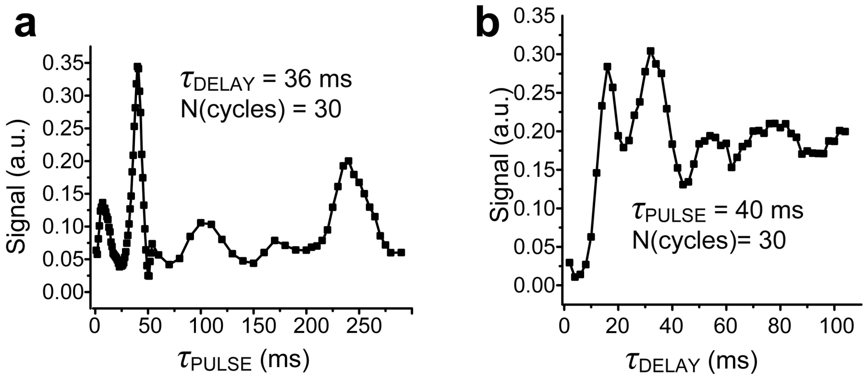

Figure S2. Supplemental pyridine-^{15}N data. The experimental conditions were the same as those using to obtain the data shown in Figure 2. a) ^{15}N QUASR-SABRE signal dependence on the duration of the shaped pulse; g) ^{15}N QUASR-SABRE signal dependence on the duration of the delay. Note the individual spectra employed for figures in displays a and b were auto-phased, and the data is presented in the magnitude mode.

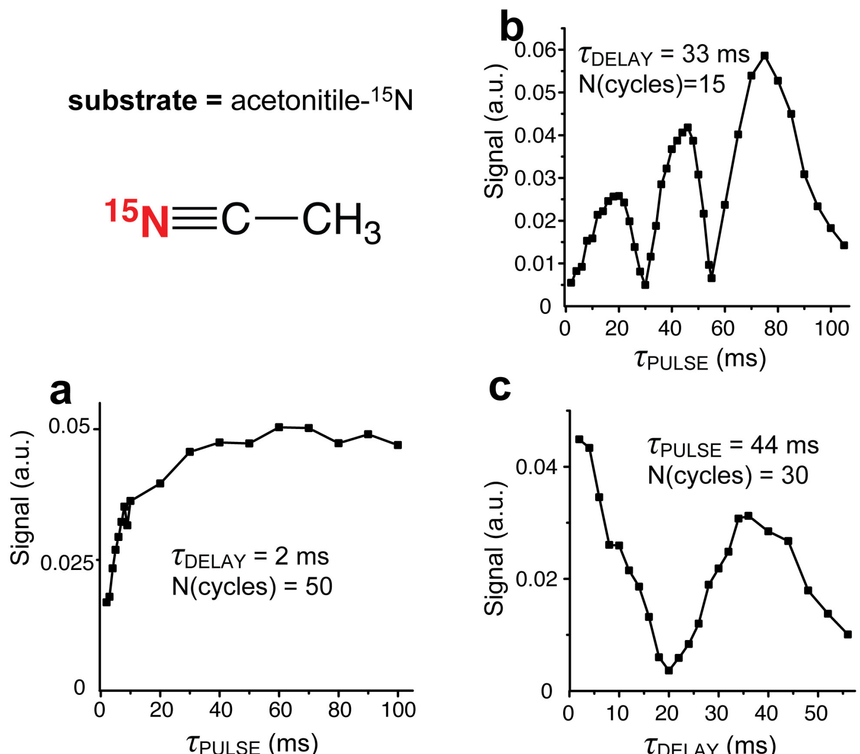

Figure S3. Supplemental acetonitrile-^{15}N data. The experimental conditions were the same as those using to obtain the data shown in Figure 3. a) ^{15}N QUASR-SABRE signal dependence on the duration of the shaped pulse; b) ^{15}N QUASR-SABRE signal dependence on the duration of the shaped pulse; c) ^{15}N QUASR-SABRE signal dependence on the duration of the delay. Note different delay duration in displays a and b.

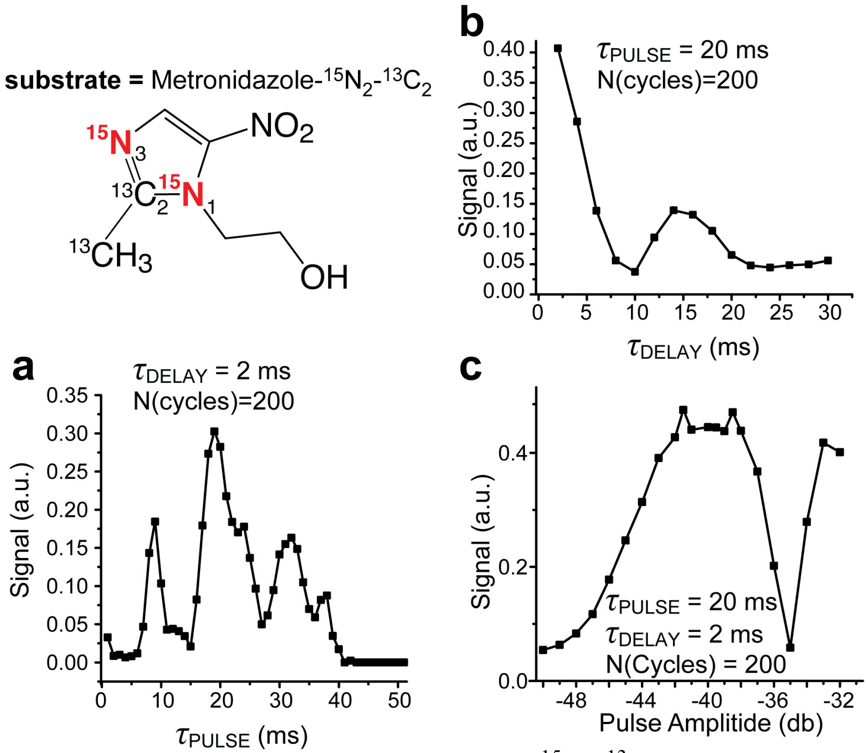

Figure S4. Supplemental metronidazole-$^{15}N_2$-$^{13}C_2$ data. The experimental conditions were the same as those using to obtain the data shown in Figure 4. a) ^{15}N QUASR-SABRE signal dependence on the duration of the shaped pulse; b) ^{15}N QUASR-SABRE signal dependence on the duration of the delay; c) ^{15}N QUASR-SABRE signal dependence on the applied radio frequency power. Note the individual spectra employed for figures in all three displays were auto-phased, and the data is presented in the magnitude mode.

3. References Used in Supporting Information

1. Shchepin, R. V.; Barskiy, D. A.; Coffey, A. M.; Feldman, M. A.; Kovtunova, L. M.; Bukhtiyarov, V. I.; Kovtunov, K. V.; Goodson, B. M.; Koptyug, I. V.; Chekmenev, E. Y. Robust Imidazole-$^{15}N_2$ Synthesis for High-Resolution Low-Field (0.05 T) ^{15}N hyperpolarized Nmr Spectroscopy. *ChemistrySelect* **2017,** *2*, 4478–4483.
2. Truong, M. L.; Shi, F.; He, P.; Yuan, B.; Plunkett, K. N.; Coffey, A. M.; Shchepin, R. V.; Barskiy, D. A.; Kovtunov, K. V.; Koptyug, I. V., et al. Irreversible Catalyst Activation Enables Hyperpolarization and Water Solubility for NMR Signal Amplification by Reversible Exchange. *J. Phys. Chem. B* **2014,** *18* 13882–13889.
3. Shchepin, R. V.; Jaigirdar, L.; Chekmenev, E. Y. Spin-Lattice Relaxation of Hyperpolarized Metronidazole in Signal Amplification by Reversible Exchange in Micro-Tesla Fields. *J. Phys. Chem. C* **2018,** *122*, 4984–4996.
4. Theis, T.; Truong, M. L.; Coffey, A. M.; Shchepin, R. V.; Waddell, K. W.; Shi, F.; Goodson, B. M.; Warren, W. S.; Chekmenev, E. Y. Microtesla Sabre Enables 10% Nitrogen-15 Nuclear Spin Polarization. *J. Am. Chem. Soc.* **2015,** *137*, 1404-1407.
5. Truong, M. L.; Theis, T.; Coffey, A. M.; Shchepin, R. V.; Waddell, K. W.; Shi, F.; Goodson, B. M.; Warren, W. S.; Chekmenev, E. Y. ^{15}N Hyperpolarization by Reversible Exchange Using SABRE-SHEATH. *J. Phys. Chem. C* **2015,** *119*, 8786–8797.